Ab initio investigation of spin orbit coupling effect on the physical properties of IrGe superconductor

H. M. Tütüncü[a,b], H. Y. Uzunok[a,b], Ertuğrul Karaca[a], S. Bağcı[a,b], G. P. Srivastava[c]

[a] *Sakarya Üniversitesi, BIMAYAM, Biyomedikal, Manyetik ve Yarıiletken Malzemeler Araştırma Merkezi, 54187, Sakarya , Turkey*

[b] *Sakarya Üniversitesi, Fen-Edebiyat Fakültesi, Fizik Bölümü, 54187, Adapazarı, Turkey*

[c] *School of Physics, University of Exeter, Stocker Road, Exeter EX4 4QL, UK*

Abstract

We have aimed to explore the influence of spin orbit coupling (SOC) on the electronic, elastic, mechanical, lattice dynamical and electron-phonon interaction properties of the simple orthorhombic IrGe using first principles density functional calculations within the generalized gradient approximation. The effect of SOC on the above properties of IrGe is mainly associated with Ir atom which possesses a 5d orbital and much heavier mass than that of Ge atom. The calculated values of nine independent elastic constants satisfy all the stability criteria, indicating that IrGe is mechanically stable in its MnP-type crystal structure. Also, no imaginary phonon frequencies are found in the phonon dispersion curves, indicating the dynamical stability of IrGe in its orthorhombic structure. Inclusion of SOC leads to the hardening of some low-frequency phonon modes which influences the electron-phonon interaction. Furthermore, inclusion of SOC leads to a decrease in dominant peaks of the Eliashberg function, and thus decrease in the values of the electron-phonon scattering parameter λ as well as the superconducting transition temperature T_c. Using the calculated value of λ with SOC, the value of T_c is obtained to be 5.09 K which compares very the recent measured value of 5.17 K.

Key words: A. intermetallics; B.density functional theory,electronic structure, superconducting properties; E. ab–initio calculations, physical properties

[1] Corresponding Author: H. M. Tütüncü Tel: +90 264 295 60 72 Fax: +90 264 295 59 50 e-Mail: tutuncu@sakarya.edu.tr

1 Introduction

Despite the discovery of unexpected high transition temperatures in oxides [1], intermetallic superconductors still continue to receive special interest. The reason for this is that the processing of high-temperature oxide compounds in the form of flexible compounds such as wires or coils is still very difficult to achieve due to their brittle, salt-like structure. Thus, intermetallic compounds are usually used as superconducting magnets and wires [2–4]. Recently, this special interest has gravitated towards intermetallic superconductors based on heavy 5d transition metals such as Ir and Pt which are chracterised by large spin orbit coupling (SOC). In recent years, several Ir-based intermetallic superconductors have been discovered by experiments. Specific heat, electrical resistivity, and magnetic susceptibility measurements [5] indicate that Ir-rich $Mg_{10}Ir_{19}B_{16}$ is a type-II superconductor at 4.45 K with an electron-phonon coupling strength (λ) of 0.66. For this superconductor [5], the density of states at the Fermi level is dominated by Ir atoms which display strong SOC in their 5d states. Thus, SOC is anticipated to play a significant role in the transition from the normal state to the superconducting state in $Mg_{10}Ir_{19}B_{16}$ due to the heavy mass of Ir atom. Two experimental groups [6,7] have reported that Li_2IrSi_3 displays type-II superconductivity with a superconducting transition temperature T_c of 3.8 K. Two theoretical calculations [8,9] made on this superconductor reveal that Ir 5d states make the main contribution to the electronic density of states close to the Fermi energy. In particular, Lu and co-workers [9] have concluded that Li_2IrSi_3 is a weak-coupling phonon-mediated superconductor. The existence of bulk superconducting transition with $T_c = 5.8$ K for the pyrochlore lattice superconductor $CaIr_2$ has been reported and the properties of this superconductor have been elucidated trough magnetization [10]. Electronic band structure calculations made on this superconductor [10] reveal that the density of states at the Fermi level is mainly dominated by the 5d states of Ir atoms. Thus, big SOC effect is expected for the physical properties of $CaIr_2$. Recently, the role of SOC on the physical properties of $CaIr_2$ has been confirmed by the *ab initio* calculations of Tütüncü and co-workers [11]. When SOC is taken into account, phonon modes in $CaIr_2$ become harder, and thus, the value of λ diminishes from 1.43 to 1.05. For this superconductor, the low-frequency phonon modes couple strongly to electrons at the Fermi level. This result is anticipated since these vibrations arise from the motion of Ir atoms and their 5d states make the largest contribution to the density of states at the Fermi level. In 2016, Okamoto and co-workers [12] reported the presence of bulk superconducting transition at 3.4 K in the ternary phosphide ScIrP. Electronic structure calculations reveal that the electronic density of states at the Fermi level is contributed by the Sc 3d and Ir 5d orbitals. Thus, SOC has the potential to effect the superconducting properties of this superconductor. This reality motivated Cuamba and co-workers [13] to study the effects of SOC on the electronic, phonon and electron-phonon interaction properties of ScIrP using a first principles method with and without SOC. When SOC is included, phonon modes become softer, and the values of λ and T_c increase for ScIrP. Haldolaarachchige and co-workers [14] have reported the synthesis and characterization of Ir-rich compound $LaIr_3$ which exhibits superconductivity below $T_c = 3.3$ K. A critical comparison of electronic band structures of $LaIr_3$ and $LaRh_3$ indicates that the Ir-rich compound has a strong SOC effect because of the heavier mass of Ir atom as compared to that of Rh atom.

Another Ir-based compound IrGe is reported to display superconductivity below $T_c = 4.7$ K [15]. This superconductor adopts the simple orthorhombic MnP-type structure. Several 4d- and 5d-

based transition metal germanides MGe (M = Rh, Pd, and Pt) have this crystal structure. The superconducting transition temperature is reported to be 0.96 K and 0.40 K for RhGe and PtGe, respectively, while PdGe is not known to superconduct above 0.4 K [15]. Thus, IrGe possesses the highest transition temperature value among its isostructural compounds. In 2013, Hirai and co-workers [16] reported a detailed characterization of IrGe and a comparison to its isostructural compounds RhGe, PdGe and PtGe. Their specific heat measurements [16] reveal that IrGe is an s-wave superconductor with a superconducting transition temperature of 5.17 K which is comparable with the earlier reported value of 4.7 [15]. Although superconductivity in IrGe has been known since 1963, neither the electronic properties nor the phonon properties of IrGe have been investigated yet. However, when studying systems in the metallic state, many physical properties, such as electrical and thermal resistivity, thermal expansion, and superconductivity, seem to be designated by phonons and their interactions with electrons. Therefore, a theoretical investigation of electron-phonon interaction in IrGe is warranted to assess the superconductivity mechanism of this compound.

In this paper, we aim to explore the structural and electronic properties of the simple orthorhombic IrGe using the *ab inito* pseudopotential method based on a generalized approximation of the density functional theory. The consideration of SOC lifts the degeneracies of some electronic bands. The second-order elastic constants are computed by imposing an external strain on the crystal, relaxing any internal parameters of the energy versus strain curve. The second order elastic constants are also effected by the inclusion of SOC. Then, phonons in IrGe have been investigated by the application of *ab initio* a linear-response scheme. Our electronic and phonon results allow us to determine the Eliashberg spectral function of IrGe, from which the average electron-phonon coupling strength is evaluated. The effect of SOC on the phonon spectrum of IrGe draws our attention. The SOC increases the frequency of some phonon modes and decreases the strength of the dominant peaks of the Eliashberg spectral function. Thus, it reduces the value of λ as well as the value of T_c. Using the calculated value of λ with SOC, the value of T_c is identified to be 5.09 K which is close to the recent measured value of 5.17 K [16].

2 Method

The calculations were performed using the the Quantum-Espresso (QE) package [17,18] based on the first-principles density functional theory (DFT) within the plane-wave pseudopotential method. The Kohn-Sham equations [19] were solved using the Perdew-Burke-Ernzerhof generalized gradient approximation (GGA) [20]. The electrostatic interaction between valence electron and ionic core was represented by the full relativistic ultrasoft pseudopotentials [21] in order to include the spin-orbit coupling. The wave function was expanded in plane waves with the energy cutoff of 60 Ry. The crystal structure of IrGe is totally relaxed by the Broyden-Fletcher-Goldfrab-Shanno optimized method [22]. The total energy changes during the optimization was finally converged to 1.0×10^{-6} eV and the forces per atom was reduced to 0.01 eV/$\mathring{A}$. Momentum space integration was carried out by using the Monkhorst-Pack special $\boldsymbol{k}$-points sampling scheme over the the irreducible part of the Brillouin-zone (IBZ) [23]. A (8×8×8) zone-centred grid was chosen to determine the structural parameters of IrGe while its electronic structure and the electronic density of states were determined with a (24×24×24) zone-centred grid.

Single-crystal elastic constants (C_{ij}) for orthorhombic IrGe are calculated using the stress-strain approach based on Hook's law: implement a suitable strain to the lattice vectors, compute the total energy against strain δ at volume V, and obtain the elastic constants from the second-order coefficient in the resulting strain. For an orthorhombic crystal, there are nine independent elastic constants, C_{11}, C_{12}, C_{13}, C_{22}, C_{23}, C_{33}, C_{44}, C_{55}, and C_{66}. These elastic constants can be calculated by using nine equations which have the following forms:

$$E(\delta) - E(0) = \frac{1}{2} C_{11} V_o \delta^2, \;\; \boldsymbol{e} = (\delta, 0, 0, 0, 0, 0) \tag{1}$$

$$E(\delta) - E(0) = \frac{1}{2} C_{22} V_o \delta^2, \;\; \boldsymbol{e} = (0, \delta, 0, 0, 0, 0) \tag{2}$$

$$E(\delta) - E(0) = \frac{1}{2} C_{33} V_o \delta^2, \;\; \boldsymbol{e} = (0, 0, \delta, 0, 0, 0) \tag{3}$$

$$E(\delta) - E(0) = \frac{1}{2} (4C_{11} - 4C_{12} - 4C_{13} + C_{22} + 2C_{23} + C_{33}) V_o \delta^2, \;\; \boldsymbol{e} = (2\delta, -\delta, -\delta, 0, 0, 0) \tag{4}$$

$$E(\delta) - E(0) = \frac{1}{2} (C_{11} - 4C_{12} + 2C_{13} + 4C_{22} - 4C_{23} + C_{33}) V_o \delta^2, \;\; \boldsymbol{e} = (-\delta, 2\delta, -\delta, 0, 0, 0) \tag{5}$$

$$E(\delta) - E(0) = \frac{1}{2} (C_{11} + 2C_{12} - 4C_{13} + C_{22} - 4C_{23} + 4C_{33}) V_o \delta^2, \;\; \boldsymbol{e} = (-\delta, -\delta, 2\delta, 0, 0, 0) \tag{6}$$

$$E(\delta) - E(0) = \frac{1}{2} C_{44} V_o \delta^2, \;\; \boldsymbol{e} = (0, 0, 0, \delta, 0, 0) \tag{7}$$

$$E(\delta) - E(0) = \frac{1}{2} C_{55} V_o \delta^2, \;\; \boldsymbol{e} = (0, 0, 0, 0, \delta, 0) \tag{8}$$

$$E(\delta) - E(0) = \frac{1}{2} C_{66} V_o \delta^2, \;\; \boldsymbol{e} = (0, 0, 0, 0, 0, \delta), \tag{9}$$

where $\boldsymbol{e}$ is the strain configuration. In this work, we compute 21 sets of $\frac{E(\delta)-E(0)}{V_o}$-$\delta$ by altering δ from -0.02 to 0.02 in steps of 0.001. Finally, our results are fitted to a parabola, and the elastic constants are derived from the quadratic coefficients.

The framework of the self-consistent density functional perturbation theory [17,18] was used to study the phonon properties of IrGe. We computed eight dynamical matrices for a 2×2×2 $\boldsymbol{q}$-point mesh within the irreducible part of the Brillouin zone. Then, they were Fourier-transformed to real space and thus the force constants obtained, which were used to get phonon frequencies for any $\boldsymbol{q}$-points. The DFT [17,18] also ensures a confident framework for implementing from first principles [17,18] the Migdal-Eliashberg approach [24–28] for determining the superconducting properties of crystals. According to the Migdal-Eliashberg theory [24,25], the Eliashberg spectral function ($\alpha^2 F(\omega)$) is defined in terms of the phonon linewidth $\gamma_{\boldsymbol{q}j}$ by

$$\alpha^2 F(\omega) = \frac{1}{2\pi N(E_F)} \sum_{\mathbf{q}j} \frac{\gamma_{\mathbf{q}j}}{\hbar \omega_{\mathbf{q}j}} \delta\left(\omega - \omega_{\mathbf{q}j}\right), \tag{10}$$

$$\gamma_{\mathbf{q}j} = 2\pi \omega_{\mathbf{q}j} \sum_{\mathbf{k}nm} |\mathrm{g}^{\mathbf{q}j}_{(\mathbf{k}+\mathbf{q})m;\mathbf{k}n}|^2 \delta(\varepsilon_{\mathbf{k}n} - \varepsilon_F) \delta(\varepsilon_{(\mathbf{k}+\mathbf{q})m} - \varepsilon_F), \tag{11}$$

where $N(E_F)$ and $\omega_{\boldsymbol{q}j}$ are the electronic density of states per atom and spin at the Fermi level and the phonon frequency, respectively, $\varepsilon_{(\mathbf{k}+\mathbf{q})m}$ and $\mathrm{g}^{\mathbf{q}j}_{(\mathbf{k}+\mathbf{q})m;\mathbf{k}n}$ are the band energies and the electron-phonon matrix elements, respectively. The matrix element for electron-phonon

interaction is

$$g^{\boldsymbol{q}j}_{(\boldsymbol{k}+q)m;\boldsymbol{k}n} = \sqrt{\frac{\hbar}{2M\omega_{\boldsymbol{q}j}}} < j, \boldsymbol{k}+qm|\Delta V^{SCF}_{\boldsymbol{q}}|i, \boldsymbol{k}n >, \tag{12}$$

where M is atomic mass and $\Delta V^{SCF}_{\boldsymbol{q}}$ denotes the derivative of the self-consistent effective potential with respect to the atomic displacements caused by a phonon with wave vector $\boldsymbol{q}$. Occasionally, it is necessary to identify a phonon mode dependent electron-phonon coupling parameter $\lambda_{\boldsymbol{q}j}$:

$$\lambda_{\mathbf{q}j} = \frac{\gamma_{\mathbf{q}j}}{\pi\hbar N(\varepsilon_F)\omega^2_{\mathbf{q}j}}. \tag{13}$$

Then, the average electron-phonon coupling λ is the summation of $\lambda_{\boldsymbol{q}j}$ over all phonon modes ($\boldsymbol{q}$j) in the IBZ,

$$\lambda = \sum_{\boldsymbol{q}j} \lambda_{\boldsymbol{q}j} W(\boldsymbol{q}), \tag{14}$$

where $W(\boldsymbol{q})$ is the weight of a sampling $\boldsymbol{q}$ point in the IBZ. The logarithmically averaged frequency $\omega_{\ln}$ has the following form [17,18,24,25,27,28]:

$$\omega_{\ln} = exp\left(\frac{1}{\lambda}\sum_{\boldsymbol{q}j} \lambda_{\boldsymbol{q}j} \ln\omega_{\boldsymbol{q}j}\right). \tag{15}$$

The Allen-Dynes modified McMillan equation [27,28] is often used to determine the superconducting temperature T_c:

$$T_c = \frac{\omega_{\ln}}{1.2}\exp\left(-\frac{1.04(1+\lambda)}{\lambda - \mu^*(1+0.62\lambda)}\right). \tag{16}$$

Here μ^* is the Coulomb pseudopotential representing Coulomb repulsion, which is taken to be 0.10 in this study. It is necessary to specify that Fermi-surface sampling for the evaluation of the electron-phonon matrix elements has been performed by using the 24×24×24 $\boldsymbol{k}$-mesh with a Gaussian width 0.015 Ry.

3 Results

3.1 Structural and Electronic Properties

IrGe possesses the simple orthorhombic MnP-type crystal structure with space group Pnma. Its primitive unit cell, depicted in Fig. 1(a), contains four formula units (eight atoms), and

each atom occupies the Wyckoff position (4c) [(x, 1/4, z)], where x and z denote the inner coordinates. This structure is thus described by three lattice parameters; a, b and c, and four inner coordinates; x_{Ir}, x_{Ge}, z_{Ir} and z_{Ge}. In order to determine these parameters, we have made the full structural optimization using the total energy minimization and zero atomic force criteria. The calculated values of the three lattice parameters and the four inner coordinates are given in Tab. 1, along with corresponding measured values [15,16]. In general, our calculated results are consistent with the experimental data [15,16]. The deviations from the recently measured values [16] of a, b and c are 0.4%, 3.0% and 0.4%, respectively. As can seen from Fig. 1(b), each atom is in six-fold coordination constituted by six atoms of the different type. The average of these six bond lengths is calculated to be 2.55 $\mathring{A}$ shorter than the sum of covalent radii for Ir and Ge 2.61 $\mathring{A}$. This result suggests that Ir and Ge atoms are bonded not only by ionic interaction, but also covalently. This feature is totally expected because the electronegativities of Ir and Ge are close to each other.

Fig. 2(a) presents the calculated electronic band structure of IrGe with and without SOC along symmetry directions of the simple orthorhombic Brillouin zone. The computed results suggest that IrGe is a three-dimensional metal with four dispersive bands crossing the Fermi level. The bonding in IrGe can be categorized as an interplay between covalent, metallic and ionic characters. The consideration of SOC in the electronic calculations causes splitting of some bands. This effect is more explicit along the X-S symmetry direction. Furthermore, the consideration of SOC changes the energies of some electronic bands, considerably. To attain an essential insight into the relationship between superconductivity observed and the electronic states of IrGe, we have calculated the total electronic density of states (DOS) and the partial electronic density of states (PDOS), which are presented in Fig. 2(b). For comparison, the total DOS without SOC is also shown in this figure. The lower valence bands arise predominantly from the Ge 4s states with lesser contribution from the other electronic states. Thus, these valence bands are nearly not effected by the inclusion of SOC. In the energy range from -6.9 to -4.8 eV, Ge 4p PDOS has the same shape as Ir 5d states which is an evidence of a strong hybridization between these states and thus of covalent interaction. Thus, p-d hybridization stabilizes the crystal structure of IrGe. Ir 5d states with strong SOC make the largest contribution to the DOS features in the range from -4.8 eV to the Fermi level. As a result, the SOC has considerable influence on the DOS features in this energy region. As electrons near the Fermi level specify the superconducting properties of solids, we have to find out their nature. The total DOS at the Fermi level ($N(E_F)$) is mainly dominated by the 5d states of Ir atoms but the contribution of Ge 4p states is also considerable. However, the contribution of Ir 5d states to $N(E_F)$ is more than two times larger than that of Ge 4p states. This result suggests that the d electrons of Ir atoms have the main contribution to the superconducting properties of IrGe, since electrons having energies close the Fermi level have the potential to form Cooper pairs in the BSC theory. Finally, the value of $N(E_F)$ with SOC is computed to be 4.747 States/eV which is lowered to 4.703 States/eV by non-inclusion of SOC.

The calculated Fermi surfaces with and without SOC are shown in Fig. 3. Because this compound has centrosymmetricity, there is no sign of antisymmetric spin-orbit coupling effect, such as 2-fold band splitting detected in the electronic band structure. Along the X-S direction, 4-fold degenerated bands are split into 2-fold degenerated bands while crossing the Fermi level. This tiny splitting can be seen in the Fermi surface with SOC in Fig. 3(d). The calculation with SOC shows significant difference on the Fermi surfaces near the Γ high symmetry point, as can

be seen in Fig. 3(b). At the Γ point, the energy differences between the 2-fold electronic bands are 0.1 eV for calculations without SOC and 0.23 eV for calculations with SOC. This energy difference could lead the discrepancy between the Fermi surface sheets that are obtained with and without SOC. Therefore, we can suggest that the effect of SOC has some influence in the electronic structure of simple orthorhombic IrGe.

3.2 Elastic and Mechanical Properties

The calculated values of the nine independent elastic constants for IrGe with and without SOC are given in Tab. 2. Unfortunately, neither experimental data nor previous theoretical values are available for comparison. Inclusion of SOC has a significant effect on the values of the nine independent elastic constants due to the existence of Ir atom which displays strong SOC in its 5d state. In particular, the maximum change is found for the value of C_{23} within 16% by inclusion of SOC. The requirement of mechanical stability [29] in a simple orthorhombic crystal lead to the following restrictions on the elastic constants:

$$C_{ii} > 0 \quad (i = 1, 6), \qquad C_{11} + C_{22} - 2C_{12} > 0, \tag{17}$$

$$C_{22} + C_{33} - 2C_{23} > 0, \qquad C_{11} + C_{33} - 2C_{13} > 0 \tag{18}$$

$$C_{11} + C_{22} + C_{33} + 2C_{12} + 2C_{13} + 2C_{23} > 0. \tag{19}$$

Obviously, the calculated elastic constants satisfy all the stability criteria, demonstrating the mechanical stability of IrGe at ambient pressure.

Once the single crystal elastic constants are calculated, the Voigt-Reuss-Hill (VHR) approach [30–32] can used to determine the polycrystalline bulk modulus (B) and shear modulus (G), Young's modulus (E) and Poisson's ratio (σ). These are fundamental parameters which are closely connected to many physical properties such as internal strain, thermoelastic stress, sound velocity, fracture, and toughness. The Voigt bulk (B_V) and shear (G_V) moduli can derived from the following equations:

$$B_V = \frac{1}{9}(C_{11} + C_{22} + C_{33} + 2C_{12} + 2C_{13} + 2C_{23}), \tag{20}$$

$$G_V = \frac{1}{15}(C_{11} + C_{22} + C_{33} + 3C_{44} + 3C_{55} + 3C_{66} - C_{12} - C_{13} - C_{23}). \tag{21}$$

The Reuss bulk (B_R) and shear (G_R) moduli are given by,

$$B_R = \frac{1}{(S_{11} + S_{22} + S_{33}) + 2(S_{12} + S_{13} + S_{23})}, \tag{22}$$

$$G_R = \frac{15}{4(S_{11} + S_{22} + S_{33}) - 4(S_{12} + S_{13} + S_{23}) + 3(S_{44} + S_{55} + S_{66})}, \tag{23}$$

where S_{ij} ($=C_{ij}^{-1}$) are the elastic compliance constants. The Hill averages of bulk (B_H) and

shear (G_H) moduli can determined by

$$B_H = \frac{B_V + B_R}{2}, \quad G_H = \frac{G_V + G_R}{2}. \tag{24}$$

Finally, the Young's modulus (E) and Poisson's ratio (σ) can derived from the following equations:

$$E = \frac{9B_H G_H}{3B_H + G_H}, \qquad \sigma = \frac{(3B_H - 2G_H)}{(6B_H + 2G_H)}. \tag{25}$$

The determined values of the isotropic bulk modulus B_{VRH}, shear modulus G_{VRH}, Young's modulus E (all in GPa), B_H/G_H ratio and Poisons's ratio σ with and without SOC for IrGe are given in Tab. 3. The value of B_{VRH}, G_{VRH}, E, B_H/G_H and σ are also affected by consideration of SOC because of changes in the values of single crystal elastic constants. For example, the value of B_R changes by 11% when SOC is taken into account. The values of B_H/G_H and σ can be used to to define the brittleness and ductility of the compound[33,34]. If these are greater than 1.75 and 0.26, respectively, the compound acts in ductile manner, and brittle otherwise. As can be seen from Tab. 3, both values of B_H/G_H and σ are larger than 1.75 and 0.26, respectively, suggesting that IrGe behaves in ductile manner. As a consequence, this superconductor is readily machinable.

Once the bulk (B_H) and shear (G_H) moduli are obtained, the longitudinal (V_L) and transverse (V_T) sound wave velocities can be calculated from the following equations [35]:

$$V_L = \left(\frac{3B_H + 4G_H}{3\rho}\right)^{1/2} \qquad V_T = \left(\frac{G_H}{\rho}\right)^{1/2}, \tag{26}$$

where ρ is the mass density of the compound. The mean sound velocity (V_M) and the Debye temperature (Θ_D)can now be calculated from [35]:

$$V_m = \left[\frac{1}{3}\left(\frac{2}{V_T^3} + \frac{1}{V_L^3}\right)\right]^{-1/3}, \qquad \Theta_D = \frac{h}{k}\left(\frac{3n}{4\pi}\frac{N_A\rho}{M}\right)^{1/3} V_m, \tag{27}$$

where h, k, n and N_A and M denote the Planck$'$s constant, Boltzmann's constant, the number of atoms in the molecule, Avogadro$'$s number and the molecular weight. The determined values of V_T, V_L, V_M and Θ_D are given in Tab. 4. When SOC is considered, the values of these quantities do not change by more than 2.3%. Thus, both calculated values of Θ_D compare very well with the corresponding value of 295.4 K [16].

3.3 Phonon and Electron-Phonon interaction Properties

The zone-centre phonon modes have special importance in the lattice dynamics of solids, as they can be analysed by different experimental techniques. The zone-centre phonons for IrGe

can be categorized by the irreducible representation of the point group D_{2h}. The group theory gives the following symmetries of the optical phonon modes:

$$\Gamma_{optic} = 4A_g + 2A_u + 4B_{3g} + 3B_{1u} + 3B_{2u} + 2B_{2g} + 2B_{1g} + B_{3u}.$$

The frequencies of the zone-centre phonon modes and their electron-phonon coupling parameters with and without SOC are presented in Tab. 5. The inclusion of SOC generates minimal amont of changes to the frequencies (ν), but the electron-phonon coupling parameters (λ) corresponding to some of the frequencies change by a large amount. When SOC is ignored, the average values of these phonon frequencies ($\overline{\nu}$) and their electron-phonon coupling parameters ($\overline{\lambda}$) are 4.37 THz and 0.028, respectively. However the consideration of SOC increases the value of $\overline{\nu}$ from 4.37 to 4.39 THz (by less than 1.0%) and decreases the value of $\overline{\lambda}$ from 0.028 to 0.023 (by 18%). Two quantities which effect mainly on λ are the phonon frequencies and electron-phonon coupling matrix elements. Since $\gamma_{\boldsymbol{q}j}$ does not depend on the phonon frequencies (see Eqs. (11) and (12)), the value of λ changes mainly with $\frac{1}{\omega^2}$ according to Eq. 13. Thus, when the frequency of phonon mode becomes harder, the value of the corresponding electron-phonon coupling parameter must be lowered. However, the increase in $\overline{\nu}$ due to SOC does not meet the decrease in $\overline{\lambda}$ due to this coupling. Consequently, a considerable decrease in $\overline{\lambda}$ must arise from decrease in the electron-phonon coupling matrix elements themselves.

A detailed identification of electron-phonon coupling requires determination of the full phonon spectrum throughout the Brillouin zone. Fig. 4(a) depicts the phonon spectrum of IrGe along high symmetry lines in the Brillouin zone of a simple orthorhombic lattice including and ignoring SOC. No imaginary phonon frequencies are present in this phonon spectrum, revealing the dynamical stability of IrGe in its MnP-type orthorhombic structure. As can be seen from Fig. 4(a), the consideration of SOC makes some low-frequency phonon modes harder which may effect the electron-phonon interaction in IrGe according to Eq. 13. The total and partial phonon density of states are shown in Fig. 4(b). Total phonon density of states without SOC is also shown in this figure for comparison. This comparison confirms the hardening of low-frequency phonon modes with the inclusion of SOC. As anticipated, Ir as the heavier element in the studied compound dominates at lower frequencies below 3.8 TH. In contrast, Ge, as the lighter element, makes much larger contribution to the higher phonon frequencies above 4.6 THz. Significant amount of Ir-Ge hybridization is present between 3.8 and 4.6 THz due to a considerable covalent interaction between these atoms.

In order to sight the strengths with which different modes of the atomic motions couple to the electrons and hence are skilful of effecting the electron-phonon interaction properties strongly, the Eliashberg spectral function $\alpha^2F(\omega)$ and the frequency dependence of the average electron-phonon coupling parameter for IrGe are displayed in Fig. 5. For comparison, the corresponding results without SOC are also shown in this figure. The SOC makes a significant influence on the property of IrGe; it weakly increases the frequency of some low-frequency phonon modes and considerably decreases the the strength of the dominant peaks of the Eliashberg spectral function. Hence, this coupling decreases the value of λ from 0.953 to 0.785. The origin of the SOC-related decrease of λ lies both in the weak hardening of some low-frequency modes and in a considerable decreases in the electron-phonon coupling matrix elements. A critical assessment of $\alpha^2F(\omega)$ with SOC reveals that the low-frequency phonon modes below 3.8 THz contribute about 76% towards λ. This huge contribution is anticipated since the heavier Ir atoms are

responsible the low frequency vibrations and their d orbitals dominate the elctronic states close to the Fermi level. From the above discussion, we can emphasize that in IrGe phonon scattering of electrons plays a considerable role in the transition from the normal state to the superconducting state. The calculated values of the physical quantities ($N(E_F)$, ω_{ln}, λ and T_c) with and without SOC related to superconductivity in IrGe are given in Tab. 6. As can be seen from this table, when SOC is included, the value of $N(E_F)$ is slightly increased from 4.703 to 4.747 (by less than 1%). However, the SOC increases the value of ω_{ln} from 101.094 to 113.857 (by around 11%). Thus, when SOC is considered, the values of λ is lowered from 0.953 to 0.785 by around 18%. Finally, SOC reduces the value of T_c from 6.523 to 5.087 K. The SOC-value of T_c agrees very well with the recent experimental value of 5.17 K [16]. We therefore emphasize that superconductivity in IrGe originates from the phonon-mediated electron-electron interaction with a medium-strength electron-phonon coupling parameter.

Finally, we have to mention that the Coulomb pseudopotential (μ^*) usually takes a value between 0.10 and 0.13 [27,28,36]. Using the Allen-Dynes formula and taking typical values of $\mu^* = 0.10$, 0.11, 0.12 and 0.13, the value of T_c with SOC (without SOC) is evaluated to be 5.087 K (6.523 K), 4.742 K (6.190 K), 4.405 (5.862 K) and 4.076 K (5.538 K), respectively. These results indicate that the value of T_c decreases when SOC is included even for different value of μ^*. The average value of T_c from the above sampling of μ^* is estimated to be 4.578 K with SOC and 6.028 K without SOC. Even these average values are comparable with the recent experimental value of 5.17 K [16]. In addition to the Allen-Dynes formula, the original form of McMillan equation can be used for the calculation of T_c. The the original form of McMillan equation is given by the following equation: [26–28]:

$$T_c = \frac{\Theta_D}{1.45} \exp\left(-\frac{1.04(1+\lambda)}{\lambda - \mu^*(1+0.62\lambda)}\right). \tag{28}$$

Using the above equation, the Debye temperature (see Tab. 4) and taking typical values of $\mu^* = 0.10$, 0.11, 0.12 and 0.13, the value of T_c with SOC (without SOC) is estimated to be 10.765 K (15.839 K), 10.035 K (15.031 K), 9.321 (14.234 K) and 8.626 K (13.448 K), respectively. All these values are very far from the experimental value of 5.17 K [16]. This result is expected because the McMillan prefactor ($\Theta_D/1.45$) is often larger than the correct prefactor ($\omega_{ln}/1.2$) [26–28,37]. As a consequence, we can suggest that the Allen-Dynes modified form of McMillan equation must be used for the calculation of T_c rather than its original form.

4 Summary

In this study, we have analysed the effect of spin orbit coupling on the electronic, elastic, mechanical, lattice dynamical and electron-phonon interaction properties of the simple orthorhombic IrGe using first principles density functional calculations within the generalized gradient approximation. The inclusion of SOC in the electronic calculations leads to the splitting of some electronic bands. The electronic density of states indicates that Ir 5d states are dominant close to the Fermi level. This finding signals that superconductivity in IrGe can be linked to the existence of Ir atom rather than the existence of Ge atom.

The calculated values of nine independent elastic constants for IrGe obey the stability criteria, indicating that IrGe is mechanically stable in its MnP-type crystal structure. The SOC has a remarkable effect on the values of nine independent elastic constants due to the existence of Ir atom which displays strong SOC in its d states. The calculated values of B_H/G_H and σ indicate the ductile character of IrGe. As a consequence, this superconductor is readily machinable.

No imaginary phonon frequencies are present in the phonon dispersion curves of IrGe, confirming its dynamical stability in the MnP-type orthorhombic structure. The inclusion of SOC leads to the hardening of some low-frequency phonon modes which influences the electron-phonon interaction. The SOC causes decrease in the dominant peaks of the Eliashberg function. The origin of the SOC-induced decrease of λ lies both in the weakly hardening of some low-frequency modes and in a significant decrease in the electron-phonon coupling matrix elements. The SOC decreases the value of λ from 0.953 to 0.785. A detailed examination of the Eliashberg function reveals that low-frequency modes below 3.8 THz contribute up to around 76% to the average electron-phonon coupling parameter λ. This result is expected because low-frequency vibrations originate from the motion of Ir atoms and their 5d states make the largest contribution to the electronic density of states at the Fermi level.

When the Allen-Dynes modified form of McMillan equation (with the Coulomb pseudopotential (μ^*)=0.11) is used, the value of T_c is found to 6.523 without SOC and 5.087 with SOC. However, these values increase to 15.839 K and 10.765 K when the original form of McMillan equation is used. The values obtained using the original form of McMillan equation is very far from the recent experimental value of 5.17 K. Thus, we can conclude that the Allen-Dynes modified form of McMillan equation gives much better result for T_c. Finally, the calculated SOC-value of T_c compares very well with the recent experimental value of 5.17 K. From our investigation, we can emphasize that the simple orthorhombic IrGe is a conventional phonon-mediated superconductor with medium-strength electron-phonon interaction.

Acknowledgement

Numerical calculations were performed using the Intel Nehalem (i7) cluster (ceres) at the University of Exeter.

References

[1] A. Schilling, M. Cantoni, J. D. Guo, H. R. Ott, Superconductivity above 130 K in the Hg–Ba–Ca–Cu–O system, Nature 363 (1993) 56-58.

[2] J. Evetts, Concise encyclopedia of magnetic and super- conducting materials, Pergamon Press, Oxford 1992.

[3] I. Pong, S. C. Hopkins, X. Fu, B. A. Glowacki, J. A. Elliott and A. Baldini, Microstructure development in Nb_3Sn(Ti) internal tin superconducting wire, Journal of Materials Science 43 (2008) 3522-3530.

[4] I. Pong, S.C. Hopkins, B.A. Glowacki, A. Baldini, Non-Uniform Bronze Formation in Internal Tin Nb_3Sn Wire, IEEE Transactions on Applied Superconductivity, 19 (2009) 2593-2597.

[5] T. Klimczuk, F. Ronning, V. Sidorov, R. J. Cava, J. D. Thompson, , Physical properties of the noncentrosymmetric superconductor $Mg_{10}Ir_{19}B_{16}$, Phys. Rev. Lett. 99 (2007) 257004.

[6] S. Pyon, K. Kudo, J.-i. Matsumura, H. Ishii, G. Matsuo, M. Nohara, H. Hojo, K. Oka, M. Azuma, V.O. Garlea, K. Kodama, S.-i. Shamoto, Superconductivity in noncentrosymmetric iridium silicide Li_2IrSi_3, J. Phys. Soc. Jpn. 83 (2014) 093706.

[7] D. Hirai, R. Kawakami, O.V. Magdysyuk, R.E. Dinnebier, A. Yaresko, H. Takagi, Superconductivity at 3.7 K in Ternary Silicide Li_2IrSi_3, J. Phys. Soc. Jpn. 83 (2014) 103703.

[8] M. Hadi, M. Alam, M. Roknuzzaman, M. Nasir, A. Islam, S. Naqib, Structural, elastic, and electronic properties of recently discovered ternary silicide superconductor Li_2IrSi_3: An ab-initio study, Chin. Phys. B 24 (2015) 117401.

[9] H. Y. Lu, N. N. Wang, L. Geng, S. Chen, Y. Yang, W. J. Lu, W. S. Wang, J. Sun, Novel electronic and phonon-related properties of the newly discovered silicide superconductor Li_2IrSi_3, EPL (Europhysics Letters) 110 (2015) 17003.

[10] N. Haldolaarachchige, Q. Gibson, L. M. Schoop, H. Luo, R. J. Cava, Characterization of the heavy metal pyrochlore lattice superconductor $CaIr_2$, J. Phys. Condens. Matter 27 (2015) 185701.

[11] H. M. Tütüncü, H. Y. Uzunok, Ertuğrul Karaca, E. Arslan, and G. P. Srivastava, Effects of spin-orbit coupling on the electron-phonon superconductivity in the cubic Laves-phase compounds $CaIr_2$ and $CaRh_2$, Phys. Rev. B 96 (2017) 134514.

[12] Y. Okamoto, T. Inohara, Y. Yamakawa, A. Yamakage, K. Takenaka, Superconductivity in the Hexagonal Ternary Phosphide ScIrP, J. Phys. Soc. Jpn. 85 (2016) 013704.

[13] A.S. Cuamba, H.-Y. Lu, C. Ting, Electronic structure and phonon-mediated superconductivity in ScIrP compound: First-principles calculations, Phys. Rev. B 94 (2016) 094513.

[14] N. Haldolaarachchige, L. Schoop, M.A. Khan, W. Huang, H. Ji, K. Hettiarachchilage, D.P. Young, Ir d-band derived superconductivity in the lanthanum-iridium system $LaIr_3$, J. Phys.: Condensed Matter 29 (2017) 475602.

[15] B. T. Matthias, T. H. Geballe, V. B. Compton, Superconductivity, Rev. Mod. Phys. 35 (1963) 1-22.

[16] D. Hirai, M. N. Ali, R. J. Cava, Strong ElectronPhonon Coupling Superconductivity Induced by a Low-Lying Phonon in IrGe, J. Phys. Soc. Jpn. 82, (2013) 124701.

[17] P. Giannozzi, S. Baroni, N. Bonini, M. Calandra, R. Car, C. Cavazzoni, D. Ceresoli, G. L. Chiarotti, M. Cococcioni, I. Dabo, A. Dal Corso, S. de Gironcoli, S. Fabris, G. Fratesi, R. Gebauer, U. Gerstmann, C. Gougoussis, A. Kokalj, M. Lazzeri, L. Martin-Samos, N. Marzari, F. Mauri, R. Mazzarello, S. Paolini, A. Pasquarello, L. Paulatto, C. Sbraccia, S. Scandolo, G. Sclauzero, A. P. Seitsonen, A. Smogunov, P. Umari, R. M. Wentzcovitch, QUANTUM ESPRESSO: a modular and open-source software project for quantum simulations of materials, J. Phys.: Condens. Matter 21 (2009) 395502.

[18] P. Giannozzi, O. Andreussi, T. Brumme, O. Bunau, M. Buongiorno Nardelli, M. Calandra, R. Car, C. Cavazzoni, D. Ceresoli, M. Cococcioni, N. Colonna, I. Carnimeo, A. Dal Corso, S. de Gironcoli, P. Delugas, R. A. DiStasio Jr., A. Ferretti, A. Floris, G. Fratesi, G. Fugallo, R. Gebauer, U.

Gerstmann, F. Giustino, T. Gorni, J. Jia, M. Kawamura, H.-Y. Ko, A. Kokalj, E. Kkbenli, M. Lazzeri, M. Marsili, N. Marzari, F. Mauri, N. L. Nguyen, H.-V. Nguyen, A. Otero-de-la-Roza, L. Paulatto, S. Ponc, D. Rocca, R. Sabatini, B. Santra, M. Schlipf, A. P. Seitsonen, A. Smogunov, I. Timrov, T. Thonhauser, P. Umari, N. Vast, X. Wu, and S. Baroni, Advanced capabilities for materials modelling with Quantum ESPRESSO, J. Phy.: Condensed Matter 29 (2017) 465901.

[19] W. Kohn, L.J. Sham, Self-consistent equations including exchange and correlation effects, Phys. Rev. 140 (1965) A1133–A1138.

[20] J.P. Perdew, K. Burke, M. Ernzerhof, Generalized gradient approximation made simple, Phys. Rev. Lett. 77 (1996) 3865–3868.

[21] A. M. Rappe, K. M. Rabe, E. Kaxiras, and J. D. Joannopoulos, Optimized pseudopotentials, Phys. Rev. B 41 (1990) 1227-1230.

[22] T.H. Fischer, J. Almlof, General methods for geometry and wave function optimization, J. Phys. Chem. 96 (1992) 9768-9774.

[23] H.J. Monkhorst, J.D. Pack, Special points for Brillouin-zone integrations, Phys. Rev. B 13 (1976) 5188–5192.

[24] A.B. Migdal, Interaction between electrons and lattice vibrations in a normal metal, Sov. Phys. JETP 34 (1958) 996.

[25] G.M. Eliashberg, Interactions between electrons and lattice vibrations in a superconductor, Zh. Eksp. Teor. Fiz. 38 (1960) 966 [Sov. Phys. JETP 11, 696(1960)].

[26] W. L. McMillan, Transition temperature of strong-coupled superconductors, Phys. Rev. 167 (1968) 331–344.

[27] P.B. Allen, R.C. Dynes, Transition temperature of strong-coupled superconductors reanalyzed, Phys. Rev. B 12 (1975) 905–922.

[28] P. B. Allen, R. C. Dynes, Superconductivity at very strong coupling, J. Phys. C. 8 (1975) L158-L163.

[29] Z.-j. Wu, E.-j. Zhao, H.-p. Xiang, X.-f. Hao, X.-j. Liu, J. Meng, Crystal structures and elastic properties of superhard IrN_2 and IrN_3 from first principles, Phys. Rev. B 76 (2007) 054115.

[30] W. Voigt, Lehrbuch der Kristallphysik, Leipzig, Taubner, (1928).

[31] A. Reuss, Berechnung der Fliegrenze von Mischkristallen auf Grund der Plastizittsbedingung fr Einkristalle, Z. Angew. Math. Mech. 9 (1929) 49.

[32] R. Hill, The elastic behaviour of a crystalline aggregate, Proceedings of the Physical Society. Section A 65 (1952) 349-354.

[33] S. Pugh, XCII. Relations between the elastic moduli and the plastic properties of polycrystalline pure metals, Phil. Mag. 45 (1954) 823-843.

[34] J. Haines, J. Leger, G. Bocquillon, Synthesis and design of superhard materials, Annu. Rev. Mater. Res. 31 (2001) 1-23.

[35] O.L. Anderson, A simplified method for calculating the Debye temperature from elastic constants, J. Phys. Chem. Solids 24 (1963) 909-917.

[36] A. P. Durajski, Influence of hole doping on the superconducting state in graphane, Supercond. Sci. Technol. 28 (2015) 035002.

[37] C. P. Poole Jr., Handbook of superconductivity, first ed.,Academic Press, San diego, 2000, Chap. 9, pp.478-489.

Table 1
The calculated values of lattice parameters (a, b and c) and internal parameters (x_{Ir}, z_{Ir}, x_{Ge}, and z_{Ge}) for IrGe and their comparison with available experimental results.

Source	$a(\mathring{A})$	$b(\mathring{A})$	$c(\mathring{A})$	x_{Ir}	z_{Ir}	x_{Ge}	z_{Ge}
This work	5.626	3.590	6.353	0.00337	0.20511	0.1894	0.5769
Experimental [15]	5.611	3.490	6.281	0.01000	0.19200	0.1850	0.5900
Experimental [16]	5.605	3.484	6.296	0.003394	0.20193	0.1875	0.5926

Table 2
The calculated values of the second order elastic constants (C_{ij} in GPa) with and without SOC for the simple orthorhombic IrGe.

Source	C_{11}	C_{12}	C_{13}	C_{22}	C_{23}	C_{33}	C_{44}	C_{55}	C_{66}
With SOC	351.82	167.74	140.62	206.97	151.67	247.94	69.43	73.53	95.96
Without SOC	364.26	154.69	134.22	184.04	128.03	233.56	71.45	77.66	97.94

Table 3
The calculated values of isotropic bulk modulus B_{VRH}, shear modulus G_{VRH}, Young's modulus E (all in GPa), B_H/G_H ratio and Poisons's ratio ν with and without SOC for IrGe, obtained from the corresponding second order elastic constants C_{ij}.

Source	B_V	B_R	B_H	G_V	G_R	G_H	E	B_H/G_H	σ
With SOC	191.87	182.95	187.41	70.89	61.55	66.22	177.74	2.83	0.342
Without SOC	179.53	163.37	171.45	73.74	64.22	68.98	182.47	2.49	0.323

Table 4
The calculated values of transverse (V_T), longitudinal (V_L), average elastic wave velocities (V_M) and Debye temperature (Θ_D) with and without SOC for the simple orthorhombic IrGe. The experimental value of Debye temperature is also given for comparison.

Source	V_T (m/s)	V_L (m/s)	V_M(m/s)	Θ_D (K)
With SOC	2198	4485	2469	291.4
Without SOC	2243	4384	2513	296.6
Experimental [16]				295.4

Table 5
Calculated zone-centre phonon modes (in THz) and their electron-phonon coupling parameters with SOC for the orthorhombic IrGe. Our results without SOC are presented in brackets. The notations I, R, and S denote infrared active, Raman active and silent modes, respectively.

Mode	ν	λ	Motion	Mode	ν	λ	Motion
B_{1g}(R)	2.10 (2.15)	0.018 (0.024)	Ir+Ge	B_{1u}(I)	5.63 (5.63)	0.007 (0.003)	Ge+Ir
A_g(R)	2.47 (2.42)	0.042 (0.069)	Ir	A_u(S)	5.84 (5.81)	0.006 (0.004)	Ge
A_u(S)	2.62 (2.58)	0.023 (0.014)	Ir+Ge	B_{3u}(I)	5.97 (5.90)	0.005 (0.002)	Ge+Ir
B_{2u}(I)	2.67 (2.55)	0.035 (0.037)	Ir+Ge	B_{2g}(R)	6.20 (6.19)	0.012 (0.014)	Ge
A_g(R)	3.07 (3.02)	0.126 (0.163)	Ir+Ge	B_{1g}(R)	6.54 (6.47)	0.006 (0.006)	Ge+Ir
B_{2g}(R)	3.26 (3.25)	0.045 (0.045)	Ir+Ge	B_{3g}(R)	6.63 (6.61)	0.024 (0.029)	Ge+Ir
B_{3g}(R)	3.89 (3.89)	0.037 (0.051)	Ir+Ge	A_g(R)	6.73 (6.68)	0.016 (0.021)	Ge+Ir
B_{3g}(R)	4.13 (4.13)	0.052 (0.069)	Ir+Ge	B_{1u}(I)	7.33 (7.33)	0.009 (0.003)	Ge+Ir
B_{1u}(I)	4.19 (4.19)	0.021 (0.011)	Ge+Ir	B_{3g}(R)	7.47 (7.45)	0.019 (0.029)	Ge
B_{2u}(I)	5.15 (5.10)	0.009 (0.012)	Ge+Ir	B_{2u}(I)	7.78 (7.84)	0.018 (0.028)	Ge
A_g(R)	5.62 (5.61)	0.033 (0.047)	Ge				

Table 6
The calculated values of physical quantities connected to superconductivity in the orthorhombic IrGe with and without SOC.

Method	$N(E_F)$ (States/eV)	ω_{ln} (K)	λ	T_c (K)
With SOC	4.747	113.957	0.785	5.087
Without SOC	4.703	101.094	0.953	6.523
Experimental [15]				4.70
Experimental [16]				5.17

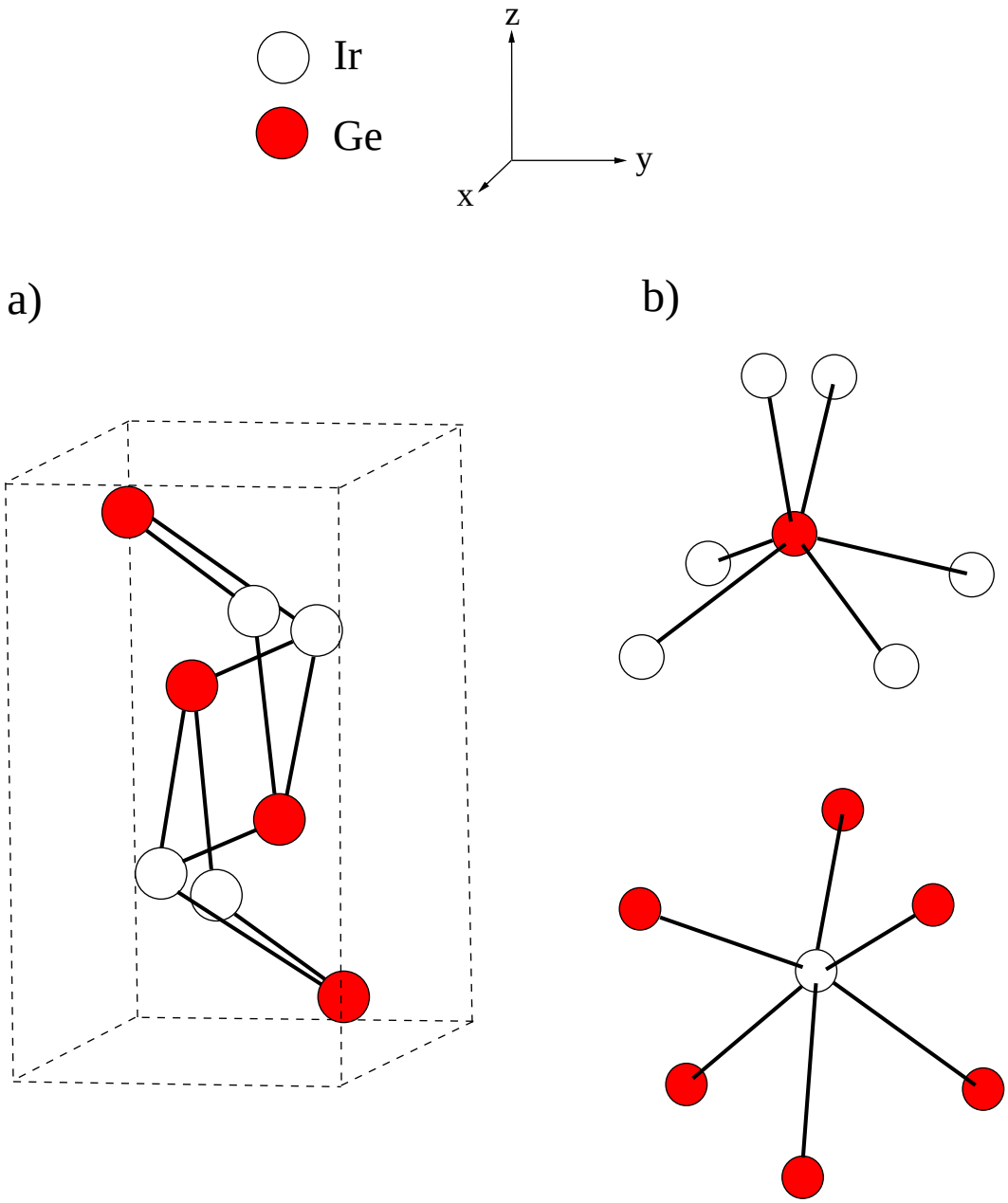

Fig. 1. (a) The simple orthorhombic MnP-type crystal structure of IrGe superconductor. (b) Each atom is surrounded by six different type atoms forming a distorted octahedron.

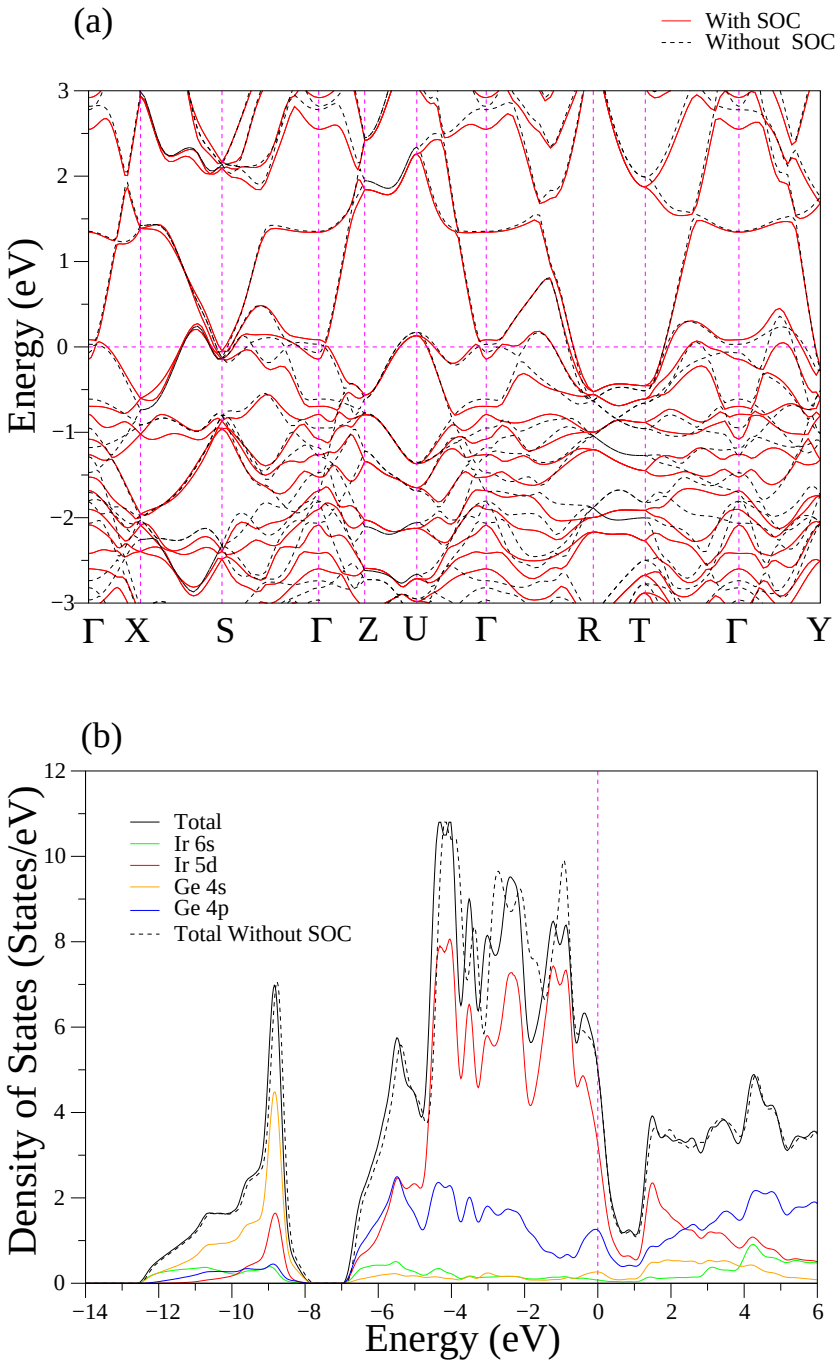

Fig. 2. (a) The electronic band structure of IrGe along specific paths of the simple orthorhombic Brillouin zone. The Fermi energy corresponds to 0 eV. (b) The total and atomic projected electronic local density of states for IrGe.

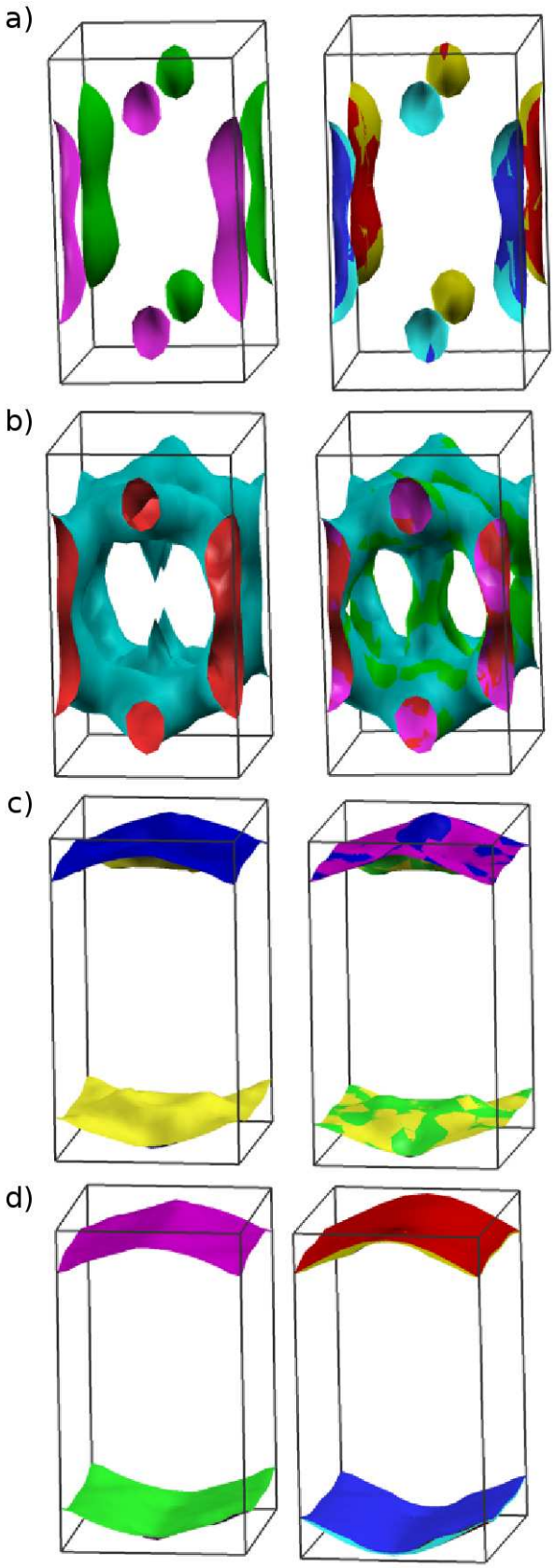

Fig. 3. The calculated Fermi surfaces of simple orthorhombic IrGe with (right panel) and without (left panel) SOC.

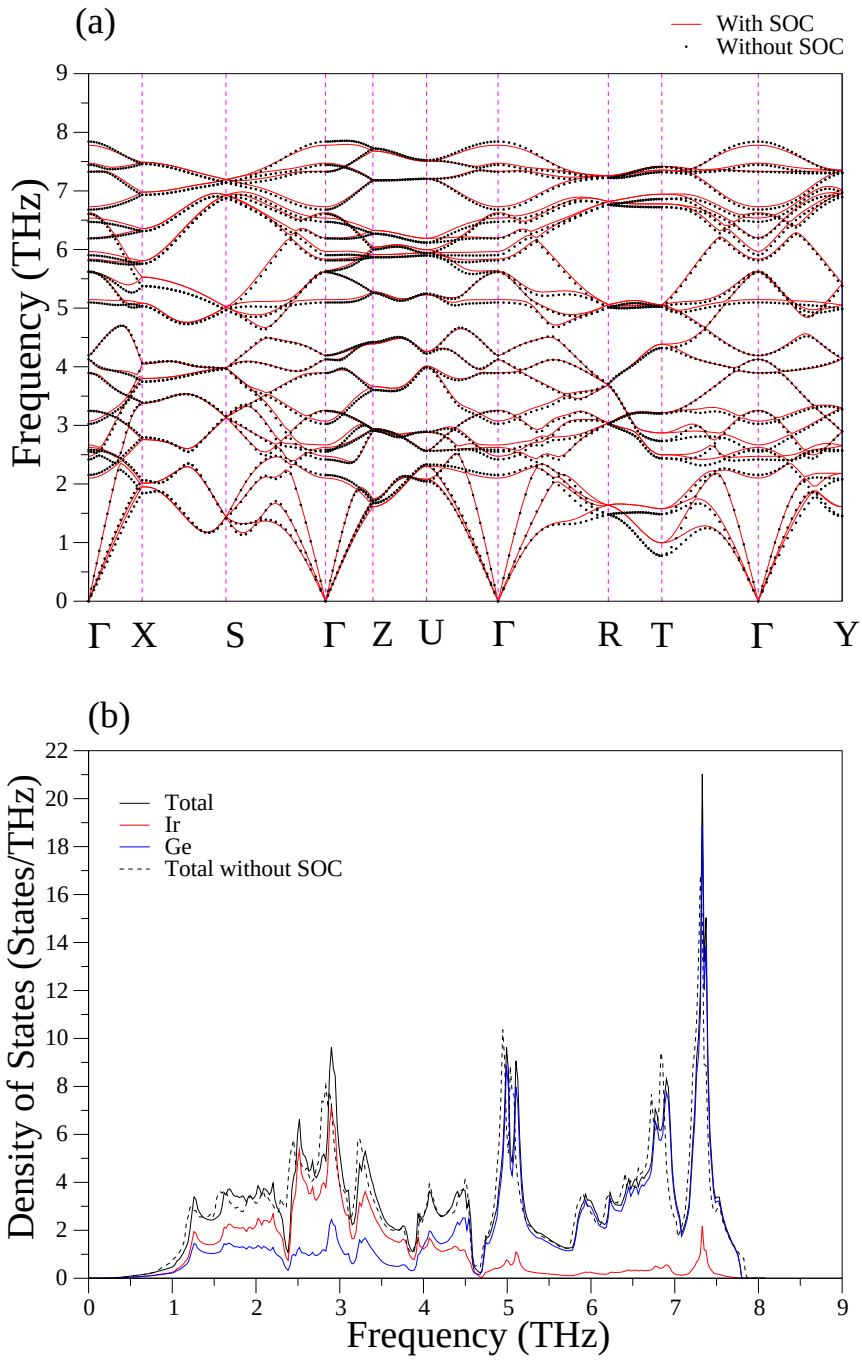

Fig. 4. (a) The phonon spectrum of IrGe along specific paths of the simple orthorhombic Brillouin zone. (b) The total and partial phonon density of states for IrGe.

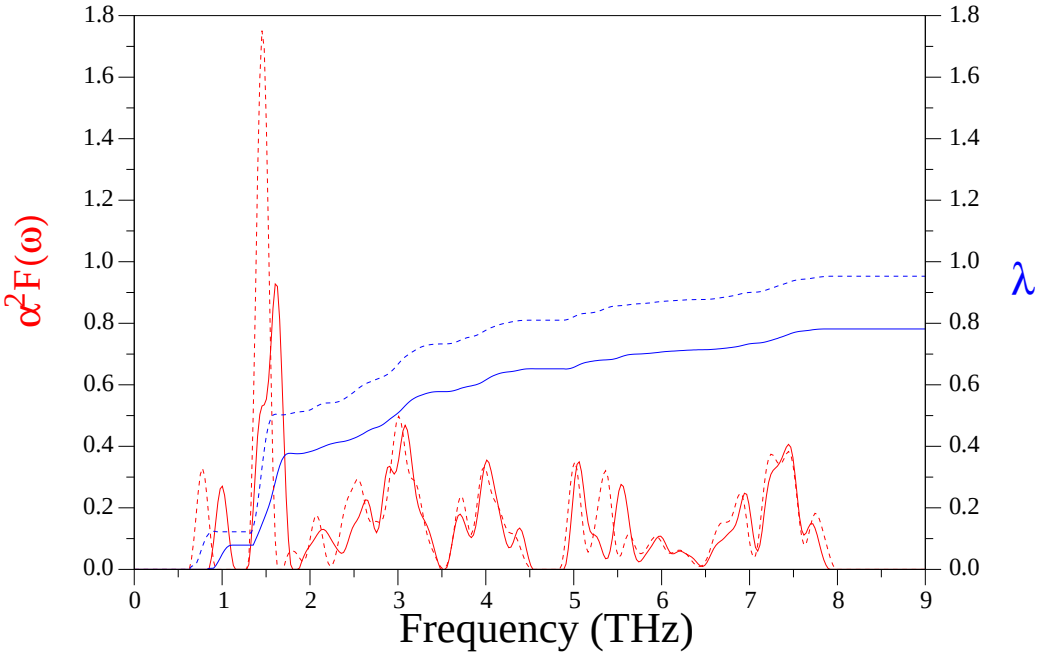

Fig. 5. Eliashberg spectral function $\alpha^2F(\omega)$ (red curve) and integrated electron-phonon coupling parameter λ (blue curve) for IrGe. The corresponding results without SOC are presented by dashed curves.